JOURNAL OF Materials CHEMISTRY

Synthesis, structure and magnetic properties of $Ln_{1-x}A_xMnO_3$ (Ln = Pr, Nd; A = Na, K) from NaCl or KCl flux†

C. Shivakumara,[a] M. S. Hegde,*[a] T. Srinivasa,[a] N. Y. Vasanthacharya,[a] G. N. Subbanna[b] and N. P. Lalla[c]

[a]*Solid State and Structural Chemistry Unit, Indian Institute of Science, Bangalore 560 012, India. Fax: +91 080 360 1310; E-mail: mshegde@sscu.iisc.ernet.in*
[b]*Material Research Center, Indian Institute of Science, Bangalore 560 012, India*
[c]*Inter-University Consortium, For DAE Facility, University Campus, Indore 452 017, India*

Received 31st May 2001, Accepted 29th June 2001
First published as an Advance Article on the web 29th August 2001

Na- or K-substituted $PrMnO_3$ and $NdMnO_3$ phases have been prepared using neutral NaCl or KCl fluxes at a relatively low temperature of 900 °C. These flux syntheses not only promote the reaction at low temperatures but also act as a source of the alkali metal in the final product. The structures of these oxides have been refined by the powder X-ray Rietveld method and confirmed by the electron diffraction studies. All these phases crystallize in the orthorhombic structure (space group *Pbnm*) and are ferromagnetic insulators. Na-doped mixed rare-earth manganites of the formula $(Pr_{1-x}La_x)_{1-y}Na_yMnO_3$ ($0 \leqslant x \leqslant 0.80$; $0.08 \leqslant y \leqslant 0.15$) have also been synthesized in NaCl flux; among these mixed rare-earth manganites those crystallizing in rhombohedral structures are ferromagnetic metals (FMM), and those in orthorhombic structures are ferromagnetic insulators (FMI). The phase diagram of average A-site radii *vs.* ferromagnetic transition temperature, T_c, of the stoichiometric phases has been constructed here and compositions with $\langle r_A \rangle \leqslant 1.20$ Å crystallizing in the orthorhombic structures fall in the ferromagnetic insulating region. Compositions with $\langle r_A \rangle \geqslant 1.20$ Å crystallize in the rhombohedral structures and these are ferromagnetic metals.

Introduction

Although $La_{1-x}A_xMnO_3$ (A = Ca, Sr, Ba and Pb) oxides showing a paramagnetic to ferromagnetic transition coupled with an insulator to metal transition have been known for nearly 50 years,[1,2] the recent observation of colossal magnetoresistance (CMR) in these oxides,[3–6] and charge ordering in the $Nd_{0.5}Sr_{0.5}MnO_3$,[7] $Pr_{1-x}Ca_xMnO_3$ ($0.3 \leqslant x \leqslant 0.5$)[8] systems has triggered new interest in the mixed valent manganite systems.[9,10] Recently alkali ion substituted lanthanum manganites have been studied in search of new systems showing CMR and related properties. Monovalent ion substituted lanthanum manganites, such as $La_{1-x}A_xMnO_3$ (A = Na, K or Rb) systems also showed properties similar to divalent ion doped mixed valent manganites.[11–14] Na- and K-doped $PrMnO_3$ systems prepared by the ceramic method have been reported by Jirak *et al.*[15,16] In this method of preparation there is an evaporative loss of Na or K ions at high temperature. The use of alkali halides as fluxes or as high-temperature solvents for the growth of crystals has been known for some time.[17] The role of the flux is generally to enhance the rate of diffusion in solid state reactions and promote the crystallization at lower temperature, and also to act as a source of the alkali metal in the final product. The flux method provides a one-step preparation for a large number of oxides, solid solutions and single crystals at relatively low temperatures. It seems to be a simple, low cost, highly reproducible and efficient technique. We have recently reported the successful synthesis of Na- and K-doped lanthanum manganites employing NaCl or KCl flux at a relatively low temperature of 900 °C.[13] Further, single crystals of Na-doped $LaMnO_3$ of 0.5–1 mm length could also be made using the NaCl flux.[18] Sodium doped rare-earth manganite perovskite crystals have also been synthesized using fused salt electrolysis.[19] Colossal magnetoresistance (CMR) was observed in an epitaxial thin film of $La_{0.82}Na_{0.13}MnO_{2.93}$,[20] and in $La_{1-x}K_xMnO_3$ in both polycrystalline[21] and thin film forms.[22] Recently, we have shown that the doping concentration of potassium in $La_{1-x}K_xMnO_3$ can be increased by increasing the oxidizing flux KCl, KBr and KI.[23] In order to see if this method can be employed to obtain alkali ion doped rare earth manganites $Ln_{1-x}A_xMnO_3$ (Ln = Pr, Nd; A = Na, K) in general, we have attempted the synthesis of such systems in NaCl or KCl flux. In this paper we report the synthesis, structure and magnetic properties of new Na- or K-doped $PrMnO_3$ and $NdMnO_3$ phases. We also show the growth of Na-doped mixed rare-earth manganites $(Pr_{1-x}La_x)_{1-y}Na_yMnO_3$ ($0 \leqslant x \leqslant 0.80$; $0.08 \leqslant y \leqslant 0.15$) in neutral NaCl flux.

Experimental

High purity La_2O_3, Nd_2O_3, Pr_6O_{11} and $MnCO_3$ were used as starting materials. The starting materials were mixed in appropriate mole ratios to realize compositions of the type Pr_yMnO_3 ($0.80 \leqslant y \leqslant 1.0$), Nd_yMnO_3 ($0.80 \leqslant y \leqslant 1.0$) and mixed rare-earth manganites of the formula $(Pr_{1-x}La_x)MnO_3$ ($0.0 \leqslant x \leqslant 0.80$). These were then ground with dry NaCl or KCl in the weight ratio 1 : 16. The mixture was heated to 900 °C for 24 h in a recrystallized alumina crucible. The melt was furnace cooled to room temperature and washed with hot distilled water, until Na^+/K^+ and Cl^- ions were absent from the filtrate. Finally, the product was dried at 110 °C in air. The flux-grown products were characterized by powder X-ray diffraction (XRD) using a Siemens D5005 diffractometer. Patterns were recorded at a scan rate of 2° min^{-1} with a Cu-Kα (1.5418 Å; Ni filter) source. X-Ray diffraction data for

†Electronic supplementary information (ESI) available: XRD patterns for $Pr_{0.92}K_{0.08}MnO_3$ and $Nd_{0.95}K_{0.05}MnO_3$ obtained by KCl melt. See http://www.rsc.org/suppdata/jm/b1/b104725f/

 DOI: 10.1039/b104725f

Table 1 Composition, lattice parameters and T_c of Na- and K-doped $PrMnO_3$ prepared by NaCl or KCl melt

Initial Pr content	Final composition	Lattice parameters/Å			Cell volume/Å^3	χ *vs.* T T_c/K
		a	*b*	*c*		
0.80	$Pr_{0.85}Na_{0.15}MnO_3$	5.4554(3)	5.4588(3)	7.7049(4)	229.45	128
0.85	$Pr_{0.90}Na_{0.10}MnO_3$	5.4563(3)	5.5031(4)	7.7060(5)	231.38	120
0.90	$Pr_{0.92}Na_{0.08}MnO_3$	5.4579(2)	5.5149(3)	7.7065(4)	231.96	100
1.00	$Pr_{0.97}Na_{0.03}Mn_{0.94}O_3$	5.4562(3)	5.5517(5)	7.6951(6)	233.09	75
0.85	$Pr_{0.92}K_{0.08}MnO_3$	5.4769(2)	5.5101(2)	7.7275(3)	233.20	145
0.90	$Pr_{0.94}K_{0.06}MnO_3$	5.4625(4)	5.5540(3)	7.7025(3)	233.68	140
1.00	$Pr_{0.98}K_{0.02}Mn_{0.94}O_3$	5.4515(6)	5.6028(5)	7.6679(7)	234.21	70

Rietveld refinement were collected from a Rigaku-2000 system with a rotating anode Cu-Kα_{12} using a graphite monochromater to filter the K$_\beta$ lines. Data were obtained at a scan rate of 1° min^{-1} with a 0.02° step size for 2θ from 10° to 100°. The data were refined using Fullprof-98. The number of parameters refined simultaneously was 30. The compositions of these oxides were obtained from chemical analysis of the elements present. Electron microscopy studies were carried out on selected samples to confirm the structure using a JEOL 200-CX transmission electron microscope. Electrical resistivity measurements were done on the sintered pellets at 900 °C by a four-probe method in the temperature range 300–15 K. DC magnetic susceptibility measurements were performed in the temperature range 300–20 K employing a Lewis coil force magnetometer (George Associates, model 2000).

Estimation of lanthanum, praseodymium and neodymium

About 100 mg of the compound was dissolved in 10 ml of 6 M HCl and evaporated to dryness. The resulting residue was redissolved in 20 ml of distilled water and 20 ml of standard 0.1 M NaF solution was added. The solution was maintained at pH 5.5 with dilute hydrochloric acid and ammonia was titrated against standard $Ln(NO_3)_3$ (Ln = La, Pr or Nd) (0.025 M) solution potentiometrically using a fluoride ion sensitive electrode (ORION: Expandable ion analyzer EA 900).[13,24] Accuracy of estimation is confirmed to be better than 0.5%. Accordingly the composition is accurate within ± 0.005.

Estimation of manganese

Typically, a known amount of the compound ($\sim$100 mg) was dissolved in 10 ml of 6 M HCl and evaporated to dryness. The resulting salt was dissolved in 20 ml of distilled water. Freshly prepared saturated sodium pyrophosphate solution (12 g of $Na_4P_2O_7{\cdot}10H_2O$ in 150 ml of H_2O) was taken and pH was adjusted to 6.5–7.0. The manganese solution was added to the well-stirred pyrophosphate solution. The resulting solution is adjusted to pH 6.5 ± 0.1. This solution was titrated against standard $KMnO_4$ (0.025 M) solution potentiometrically using Pt and calomel electrode.[25] At pH 6.7, there is no interference of La, Pr and Nd ions. Estimation of Mn is accurate within ± 0.01.

Estimation of sodium and potassium

Sodium and potassium contents were estimated by flame photometry. About 100 mg of compounds were dissolved in 5 ml of 6 M HCl, evaporated to dryness and redissolved in 100 ml of de-ionized water. Standard solutions were prepared from analytical grade (AR) NaCl and KCl salts dried at 200 °C. The accuracy of estimation is within ± 0.01.

Determination of oxygen content

The oxygen content was determined by iodometric titration. The procedure involves a known quantity of a sample (50–100 mg) dissolved in 10 ml of 6 M HCl containing 2 g of KI. Liberated iodine was titrated against standard sodium thiosulfate (0.05 M) solution using starch as an indicator. The oxygen content in the formula reported here is accurate within ± 0.02.

Results

$Pr_{1-x}Na_xMnO_3$

With the initial Pr concentration in the range of 0.80 to 0.90 with respect to Mn, stoichiometric $Pr_{1-x}Na_xMnO_3$ could be obtained. The variation in Na content, x, was 0.15 to 0.03. In order to see if more of Na can be substituted by this method, a Pr to Mn ratio of 0.75 : 1.0 was used for a preparation. The X-ray diffraction pattern of the product showed Mn_3O_4 as an impurity phase along with sodium substituted $PrMnO_3$. Thus, the maximum amount of sodium that could be substituted was 0.15. However, when the initial Pr to Mn ratio was 1 : 1, the Na content was low ($x = 0.03$) but, elemental analysis showed an Mn deficiency to the extent of 6%. The compositions and refined lattice parameters of Na-doped $PrMnO_3$ phases are summarized in Table 1.

The structures of sodium substituted $PrMnO_3$ phases were refined by powder X-ray Rietveld analysis. The compounds crystallize in the orthorhombic structure (space group *Pbnm* no. 62). Observed, calculated and difference X-ray diffraction patterns for $Pr_{0.85}Na_{0.15}MnO_3$ are given in Fig. 1 and there is good agreement between the observed and calculated patterns. The refined structural parameters of all the phases are summarized in Table 2. In all, 30 parameters (overall scale factor, background, unit cell and thermal parameters) were varied simultaneously for the experimental composition. From Table 2, we can see that the orthorhombic distortion systematically increases with decreasing Na ion concentration. This is reflected in the decrease of the Mn–O–Mn bond angles. The cell volume also increases with decreasing Na ion doping.

When a Pr to Mn ratio of 1 : 1 was adopted in the preparation, the final composition obtained was $Pr_{0.97}Na_{0.03}Mn_{0.94}O_3$

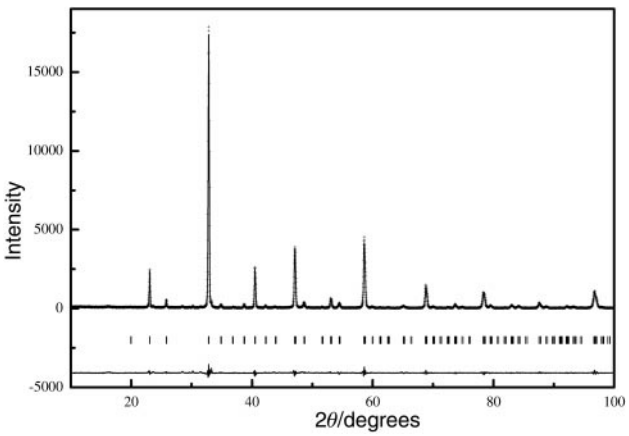

Fig. 1 Observed (+), calculated (solid line) and difference (bottom) X-ray diffraction patterns for $Pr_{0.85}Na_{0.15}MnO_3$ obtained by NaCl melt.

Table 2 Structural and thermal parameters (B) of Na-doped $PrMnO_3$ obtained by NaCl melt

	$Pr_{0.85}Na_{0.15}MnO_3$	$Pr_{0.90}Na_{0.10}MnO_3$	$Pr_{0.92}Na_{0.08}MnO_3$	$Pr_{0.97}Na_{0.03}Mn_{0.94}O_3$
Pr/Na (x, y, 0.25)				
x	−0.0052(4)	−0.0051(6)	−0.0064(3)	−0.0073(3)
y	0.0278(1)	0.0345(2)	0.0381(2)	0.0440(1)
B/Å^2	0.81	0.75	0.63	0.58
Mn (0.5, 0, 0)				
B/Å^2	0.55	0.53	0.50	0.45
O(1) (x, y, 0.25)				
x	0.0690(3)	0.0657(3)	0.0702(2)	0.0822(2)
y	0.4828(2)	0.4876(2)	0.4861(2)	0.4816(2)
B/Å^2	0.62	0.45	0.56	0.73
O(2) (x, y, z)				
x	−0.2735(3)	−0.2736(3)	−0.2794(9)	−0.2803(2)
y	0.2902(2)	0.2941(2)	0.2885(6)	0.2891(6)
z	0.0368(5)	0.03931(3)	0.0411(8)	0.0428(9)
B/Å^2	0.76	0.53	0.48	0.62
Lattice parameters/Å				
a	5.4554(3)	5.4563(3)	5.4579(2)	5.4562(3)
b	5.4588(3)	5.5031(3)	5.5149(3)	5.5517(3)
c	7.7049(4)	7.7060(5)	7.7065(4)	7.6951(4)
R factors (%)				
R_p	7.17	11.3	9.32	8.85
R_{wp}	10.2	12.6	12.2	11.7
R_{Bragg}	2.70	7.23	4.66	4.74
Bond lengths/Å				
Mn–O(1)	1.964(9)	1.961(1)	1.965(8)	1.978(3)
Mn–O(2)	1.902(2)	1.897(6)	1.945(8)	1.954(1)
Mn–O(2)′	2.029(1)	2.060(7)	2.020(2)	2.030(1)
Bond angles/°				
Mn–O(1)–Mn	157.2(2)	158.6(7)	157.0(7)	153.1(1)
Mn–O(2)–Mn	157.9(6)	156.5(5)	156.0(1)	155.3(2)

indicating Mn-site vacancy. This phase also crystallizes in the same *Pbnm* space group and the structure refines well with 6% Mn deficiency. When the Mn-site occupancy is increased from the experimental value of 0.94 to 1.0, while keeping all other parameters the same, R_{Bragg} increased from 4.74% to 5.5%, suggesting the presence of a Mn-site vacancy in the compound. A similar Mn-site deficient phase $La_{0.98}Na_{0.02}Mn_{0.92}O_3$ was obtained in the $LaMnO_3$ system when the La : Mn ratio was 1 : 1.[13]

$Pr_{1-x}K_xMnO_3$

The composition and the refined lattice parameters of K-doped $PrMnO_3$ are summarized in Table 1. The structures of these phases have been refined and they also crystallize in the orthorhombic structure with *Pbnm* space group. Observed, calculated and difference X-ray patterns are deposited as ESI.† In Table 3, the structural parameters are summarized. As can be seen from Table 3, reasonably good fitting is obtained. The orthorhombicity increases with decreasing potassium ion doping as reflected in the decrease in Mn–O–Mn bond angles.

When the initial Pr to Mn ratio was 0.8 : 1.0, Mn_3O_4 as an impurity phase was observed in the XRD pattern. However, with increasing Pr to Mn ratio, the extent of K ion doping decreased. The maximum K-ion substitution for Pr obtained was 0.08. Chemical analysis and refinement of X-ray data indicate Mn-site vacancy when the Pr to Mn initial ratio of 1 : 1 is adopted in the preparation. As much as 6% Mn-site vacancy is observed. This compound also crystallizes in the same *Pbnm* space group.

$Nd_{1-x}A_xMnO_3$ (A = Na, K)

Na- and K-doped $NdMnO_3$ have been synthesized in NaCl or KCl fluxes for the first time. These oxides also crystallize in the orthorhombic structure with the *Pbnm* space group. In Table 4, the compositions, refined lattice parameters and cell volumes are summarized. Observed, calculated and difference X-ray diffraction patterns for $Nd_{0.95}K_{0.05}MnO_3$ are deposited as ESI.† The structural parameters of all the compounds are summarized in Table 5. The maximum amount of Na ion that could be doped was 0.11. Relatively less K could be doped compared to Na ion in the $PrMnO_3$ and $NdMnO_3$ systems. With increasing Nd : Mn ratio, the extent of doping of Na or K decreased and the orthorhombicity increased. Here also, stoichiometric $Nd_{1-x}A_xMnO_3$ could be obtained for the initial Nd : Mn ratio in the range 0.85 to 0.90. With 1 : 1 ratio, Mn-site deficient compounds were obtained.

$(Pr_{1-x}La_x)_{1-y}Na_yMnO_3$

Synthesis of Na-doped mixed rare-earth manganites by NaCl flux has also been carried out. Initial composition corresponding to $(Pr_{1-x}La_x)_{0.8}MnO_3$ was taken and the Pr to La ratio was varied. With $La_{0.8}MnO_3$ initial concentration, the final product obtained is $La_{0.90}Na_{0.09}MnO_3$ which crystallizes in the rhombohedral structure. This is why we chose the initial ratio of Ln : Mn of 0.8 : 1.0. By varying the Pr to La ratio, stoichiometric Na-doped mixed rare-earth manganites could be prepared in NaCl flux. The compositions and lattice parameters of these oxides are summarized in Table 6 and their X-ray diffraction patterns are shown in Fig. 2. The end members $La_{0.90}Na_{0.09}MnO_3$ and $Pr_{0.85}Na_{0.15}MnO_3$ crystallized in rhombohedral and orthorhombic structures respectively. Accordingly, as the Pr to La ratio increased, the structure changed from rhombohedral to orthorhombic symmetry. Thus, Na-doped mixed rare-earth manganites can also be prepared in NaCl flux.

Table 3 Structural and thermal parameters (B) of K-doped $PrMnO_3$ obtained by KCl melt

	$Pr_{0.92}K_{0.08}MnO_3$	$Pr_{0.94}K_{0.06}MnO_3$	$Pr_{0.98}K_{0.02}Mn_{0.94}O_3$
Pr/K (x, y, 0.25)			
x	−0.0059(3)	−0.0075(2)	−0.0083(4)
y	0.0325(1)	0.0402(4)	0.0479(2)
B/Å^2	0.65	0.83	0.79
Mn (0.5, 0, 0)			
B/Å^2	0.26	0.33	0.20
O(1) (x, y, 0.25)			
x	0.0685(4)	0.0762(5)	0.0876(3)
y	0.4844(6)	0.4735(8)	0.4644(5)
B/Å^2	0.32	0.45	0.62
O(2) (x, y, z)			
x	−0.2743(3)	−0.2748(8)	−0.2752(9)
y	0.2934(7)	0.2905(5)	0.2892(6)
z	0.0368(6)	0.0402(5)	0.0440(5)
B/Å^2	0.49	0.56	0.38
Lattice parameters/Å			
a	5.4769(2)	5.4625(4)	5.4515(6)
b	5.5101(2)	5.5540(3)	5.6028(5)
c	7.7275(3)	7.7025(6)	7.6679(7)
R factors (%)			
R_p	8.9	10.2	11.4
R_{wp}	12.2	12.5	13.7
R_{Bragg}	4.39	6.50	5.89
Bond lengths/Å			
Mn–O(1)	1.969(8)	1.973(7)	1.985(6)
Mn–O(2)	1.906(2)	1.924(5)	1.938(9)
Mn–O(2)′	2.054(9)	2.052(6)	2.059(4)
Bond angles/°			
Mn–O(1)–Mn	157.4(6)	153.7(1)	149.8(1)
Mn–O(2)–Mn	157.4(1)	158.1(9)	155.6(7)

Electron microscopic studies

Scanning electron microscopy (SEM) of these oxides was carried out for morphology and possible detection of impurity phases. The compositional homogeneity of many particles was checked by energy dispersive X-ray (EDX) analysis in spot mode and they were close to the final composition reported in Tables 1 and 4. A typical scanning electron micrograph of $Pr_{0.9}Na_{0.1}MnO_3$ is shown in Fig. 3. Crystals of cubic morphology are evident from the picture.

Detailed electron diffraction studies on Na- or K-doped $PrMnO_3$ and $NdMnO_3$ systems were carried out in a transmission electron microscope (TEM) to elucidate the crystal structure and to investigate the possible cation ordering. These oxides crystallize in the orthorhombic structure related to $GdFeO_3$. The typical selected area electron diffraction (SAED) pattern recorded along the (100) direction for $Pr_{0.85}Na_{0.15}MnO_3$ is shown in Fig. 4(a). In Fig. 4(b) and (c) we show the SAED patterns recorded along the (100) and (110) directions for $Nd_{0.95}K_{0.05}MnO_3$. The lattice parameters obtained from electron diffraction studies agree well with the X-ray studies. However we could not see superlattice reflections corresponding to the cation ordering indicating that Na- or K-ions are randomly distributed.

Magnetic properties

In Fig. 5, the magnetic susceptibilities of Na-doped $PrMnO_3$ as a function of temperature are presented. These oxides showed a paramagnetic to ferromagnetic transition. The transition temperature, T_c, decreases with decreasing sodium content. A maximum T_c of 128 K is observed for the compound $Pr_{0.85}Na_{0.15}MnO_3$. The χ^{-1} *vs.* T plot in general showed Curie–Weiss behaviour. The inset (Fig. 5) shows a typical χ^{-1} *vs.* T plot for the stoichiometric compound $Pr_{0.90}Na_{0.10}MnO_3$. The T_c's of the Na-doped $PrMnO_3$ are summarized in Table 1.

The magnetic susceptibilities of K-doped $PrMnO_3$ as a function of temperature also showed similar behavior to the Na-doped compounds. The ferromagnetic transition temperature, T_c, decreases with decreasing potassium content. The maximum T_c of 145 K was observed in $Pr_{0.92}K_{0.08}MnO_3$. In Table 1, the T_c values of the K-doped $PrMnO_3$ are summarized.

Temperature dependent magnetic susceptibility measurements of Na- and K-doped $NdMnO_3$ have also been carried out. All the compounds show paramagnetic to ferromagnetic transitions. Here also, the ferromagnetic transition temperature, T_c, decreased with decreasing Na or K content. The T_c's

Table 4 Composition, lattice parameters and T_c of Na- and K-doped $NdMnO_3$ prepared by NaCl or KCl melt

		Lattice parameters/Å				
Initial Nd content	Final composition	a	b	c	Cell volume/Å^3	χ *vs.* T T_c/K
0.85	$Nd_{0.89}Na_{0.11}MnO_3$	5.4313(4)	5.5218(4)	7.6697(6)	230.02	118
0.90	$Nd_{0.94}Na_{0.06}MnO_3$	5.4202(2)	5.5910(2)	7.6423(3)	231.59	95
1.00	$Nd_{0.98}Na_{0.02}Mn_{0.91}O_3$	5.4143(7)	5.6367(6)	7.6263(9)	232.75	70
0.90	$Nd_{0.95}K_{0.05}MnO_3$	5.4397(6)	5.6242(5)	7.6351(3)	233.58	95
1.00	$Nd_{0.98}K_{0.02}Mn_{0.91}O_3$	5.4158(5)	5.6563(5)	7.6223(7)	233.49	70

Table 5 Structural and thermal parameters of Na- and K-doped $NdMnO_3$ prepared by NaCl or KCl flux

	$Nd_{0.89}Na_{0.11}MnO_3$	$Nd_{0.98}Na_{0.02}Mn_{0.91}O_3$	$Nd_{0.95}K_{0.05}MnO_3$	$Nd_{0.98}K_{0.02}Mn_{0.91}O_3$
Nd/Na (x, y, 0.25)				
x	−0.0066(6)	−0.0099(4)	−0.0091(5)	−0.0103(5)
y	0.0425(2)	0.0535(2)	0.0502(2)	0.0544(2)
B/Å^2	0.41	0.79	0.73	0.69
Mn (0.5, 0, 0)				
B/Å^2	0.66	0.54	0.52	0.38
O(1) (x, y, 0.25)				
x	0.0847(4)	0.1037(3)	0.0859(9)	0.1121(3)
y	0.4842(3)	0.4567(6)	0.4586(8)	0.4488(5)
B/Å^2	0.62	0.55	0.44	0.59
O(2) (x, y, z)				
x	−0.2647(4)	−0.2728(3)	−0.2764(3)	−0.2699(3)
y	0.2953(8)	0.3021(2)	0.29496)	0.3015(2)
z	0.0459(8)	0.0376(6)	0.0427(2)	0.0353(5)
B/Å^2	0.44	0.38	0.52	0.41
Lattice parameters/Å				
a	5.4313(4)	5.4143(7)	5.4397(6)	5.4158(5)
b	5.5218(4)	5.6367(6)	5.6242(5)	5.6563(5)
c	7.6697(5)	7.6263(9)	7.6351(3)	7.6223(7)
R factors (%)				
R_p	11.6	10.0	10.6	11.7
R_{wp}	12.8	12.9	12.2	13.2
R_{Bragg}	7.75	6.45	5.98	6.60
Bond lengths/Å				
Mn–O(1)	1.974(8)	2.001(1)	1.978(9)	2.021(1)
Mn–O(2)	1.862(4)	1.870(2)	1.922(7)	1.862(9)
Mn–O(2)′	2.101(3)	2.122(2)	2.082(6)	2.129(1)
Bond angles/°				
Mn–O(1)–Mn	152.55	144.37	149.39	141.09
Mn–O(2)–Mn	155.33	156.32	155.22	157.49

of Na- and K-doped $NdMnO_3$ phases are summarized in Table 4.

In the case of $(Pr_{1-x}La_x)_{1-y}Na_yMnO_3$ system T_c varies with varying Pr to La ratio. The maximum T_c of 310 K is observed for the composition $La_{0.90}Na_{0.09}MnO_3$, and with increasing Pr content T_c decreases. In Table 6, T_c values are summarized.

Electrical properties

Four-probe electrical resistivity as a function of temperature was measured on the sintered pellets. No measurable change in the composition of the sintered pellets is seen with respect to the unsintered samples. All the Na- or K-doped $PrMnO_3$ and $NdMnO_3$ samples were semiconducting. The band gaps, E_g, of these oxides were calculated from the slope of ln ρ *vs.* T^{-1} plots. The band gaps are in the range of 0.056–0.077 eV.

In the case of the $(Pr_{1-x}La_x)_{1-y}Na_yMnO_3$ system, compounds crystallizing in the rhombohedral structure showed a metal to insulator (M–I) transition coupled with a paramagnetic to ferromagnetic transition (see Table 6). With increasing Pr content in the mixed rare-earth manganite system, the structure changed from rhombohedral to orthorhombic symmetry and the compounds crystallizing in the orthorhombic structure were semiconducting. A typical resistivity *vs.* temperature plot of $(PrLa)_{0.85}Na_{0.15}MnO_3$ is given in Fig. 6. In the inset, the ln ρ *vs.* T^{-1} plot of $(PrLa)_{0.91}Na_{0.09}MnO_3$ is given.

Discussion

The primary aim of this study was to prepare stoichiometric Na- or K-doped $PrMnO_3$ and $NdMnO_3$ phases employing neutral NaCl or KCl flux. In the alkali halide flux synthesis not only does the reaction occur at low temperatures but the flux acts as a source of the alkali metal in the final product. Therefore, to force Na- or K doping for Pr or Nd-sites, the initial ratio of Pr : Mn or Nd : Mn has to be less than 1. Accordingly, when a Pr to Mn ratio of 0.8 : 1.0 was taken in the preparation, the final composition obtained was $Pr_{0.85}Na_{0.15}MnO_3$. The excess Mn seems to be converted into a soluble manganese salt, since we do not see any detectable manganese oxides impurity phases in the X-ray diffraction patterns or SEM/EDX studies. As the Pr to Mn ratio increased from 0.8 : 1.0 to 1 : 1, partial conversion of Mn to soluble salts

Table 6 Composition, lattice parameters, electrical and magnetic properties of $(Pr_{1-x}La_x)_{1-y}Na_yMnO_3$ prepared by NaCl flux

Initial La content	Final composition	Crystal structure[a]	Lattice parameters/Å			R *vs.* T T_{I-M}/K	χ *vs.* T T_c/K
			a	b	c		
0.00	$Pr_{0.85}Na_{0.15}MnO_3$	O	5.462(2)	5.455(2)	7.699(2)	Insulator	128
0.20	$(PrLa)_{0.92}Na_{0.08}MnO_3$	O	5.471(2)	5.505(4)	7.728(3)	Insulator	130
0.40	$(PrLa)_{0.91}Na_{0.09}MnO_3$	O	5.485(4)	5.488(4)	7.769(1)	Insulator	135
0.60	$(PrLa)_{0.85}Na_{0.15}MnO_3$	R	5.511(3)	—	13.354(4)	232	300
0.80	$La_{0.90}Na_{0.09}MnO_3$	R	5.522(2)	—	13.354(3)	240	310

[a]R = Rhombohedral, O = Orthorhombic.

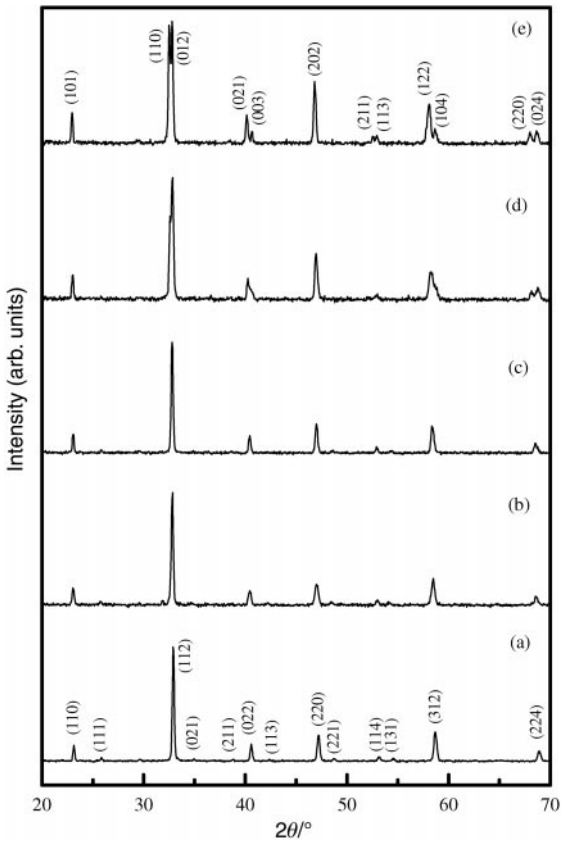

Fig. 2 Powder X-ray diffraction patterns of (a) $Pr_{0.85}Na_{0.15}MnO_3$, (b) $(PrLa)_{0.92}Na_{0.08}MnO_3$, (c) $(PrLa)_{0.91}Na_{0.09}MnO_3$, (d) $(PrLa)_{0.85}Na_{0.15}MnO_3$, (e) $La_{0.90}Na_{0.09}MnO_3$.

can lead to the formation of Mn-deficient phases. Indeed, the chemical analysis and the X-ray refinement data support the formation of an Mn-deficient $Pr_{0.97}Na_{0.03}Mn_{0.94}O_3$ phase in NaCl flux. When excess Mn was taken in the preparation, *viz.* a Pr to Mn ratio of 0.75 : 1.0, a Mn_3O_4 impurity was observed in the X-ray diffraction pattern. Thus, stoichiometric Na- or K-doped $PrMnO_3$ and $NdMnO_3$ can be obtained in a narrow range of initial dopant content of 0.8 to 0.9 with respect to Mn. It is to be noted that even in this narrow range of initial composition, the extent of Na- or K-doping can be varied.

In the KCl flux method, the extent of K-ion substitution achieved is only about 0.08 as against 0.15 reported by Jirak *et al.*[15] Relatively less K could be doped compared to Na in the $PrMnO_3$ as well as $NdMnO_3$ systems. This is probably due to the larger difference in the ionic radii between Nd^{3+} ($r_{Nd} = 1.163$ Å) and K^+ ($r_K = 1.55$ Å) compared to Na^+ ($r_{Na} = 1.24$ Å). In the $PrMnO_3$ system also, less K^+ could be substituted for Pr^{3+} ($r_{Pr} = 1.179$ Å) ion compared to Na^+ as can be seen from Table 1. Further, the lattice parameters of

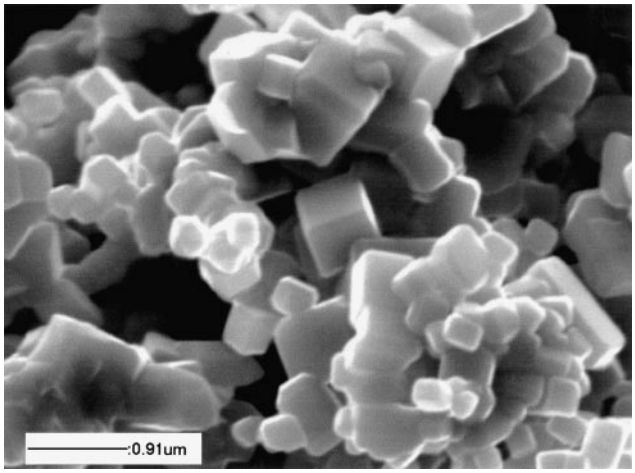

Fig. 3 Typical scanning electron micrograph of $Pr_{0.90}Na_{0.10}MnO_3$.

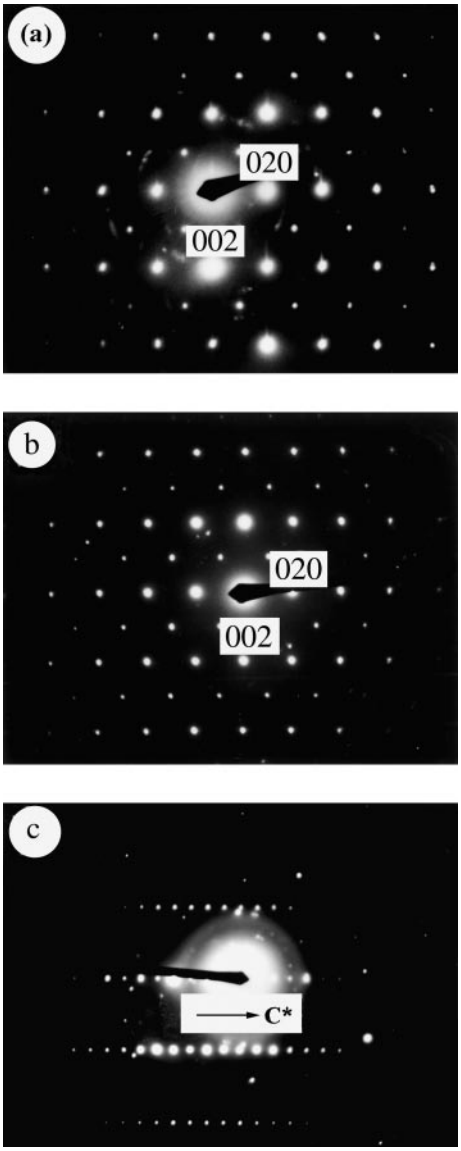

Fig. 4 Selected area electron diffraction patterns of (a) $Pr_{0.85}Na_{0.15}MnO_3$ prepared from the NaCl flux recorded along the (100) direction, and $Nd_{0.95}K_{0.05}MnO_3$ prepared from the KCl flux recorded along the (b) (100) and (c) (110) directions.

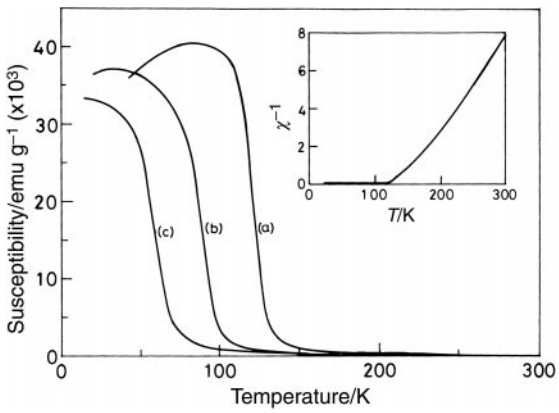

Fig. 5 Magnetic susceptibility plots as a function of temperature for (a) $Pr_{0.90}Na_{0.10}MnO_3$, (b) $Pr_{0.91}Na_{0.09}MnO_3$, (c) $Pr_{0.97}Na_{0.03}Mn_{0.94}O_3$. Inset shows the χ^{-1} *vs.* T plot of $Pr_{0.90}Na_{0.10}MnO_3$.

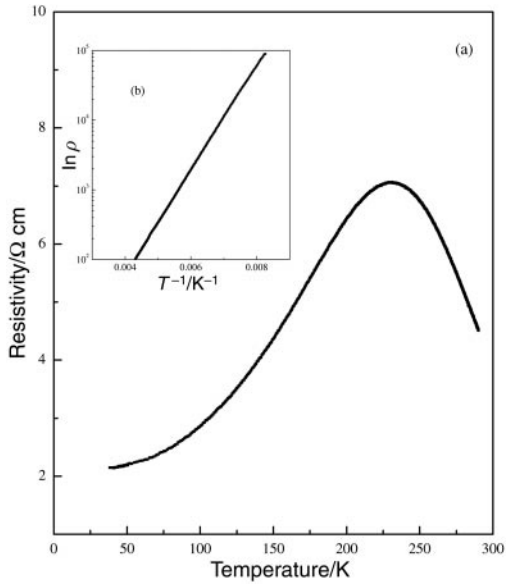

Fig. 6 Temperature dependent resistivity plot of $(PrLa)_{0.85}Na_{0.15}MnO_3$. Inset shows the ln ρ *vs.* T^{-1} plot of $(PrLa)_{0.91}Na_{0.09}MnO_3$.

$Nd_{0.95}K_{0.05}MnO_3$ are close to those of $NdMnO_3$ reported by Cherepanov *et al.*[26]

Na- or K-doped $PrMnO_3$ and $NdMnO_3$ systems crystallize in orthorhombic structures. The Goldschmidt tolerance factors $[t=(r_A+r_O)/\sqrt{2}(r_B+r_O)]$ for these compositions were calculated using the average radius $\langle r_A\rangle$ (Shannon value for 9-fold coordination).[27] The ionic radii of Mn and oxide ions used were 0.645 Å and 1.35 Å respectively. The t values are in the range of 0.88–0.93. Therefore these oxides are expected to crystallize in the orthorhombic structure.

In $LaMnO_3$ system, $La_{1-x}MnO_{3-\delta}$ with A-site as well as oxygen site vacancies and $LaMn_{1-x}O_3$ with Mn-site vacancy have been reported by Topfer and Goodenough.[28] While $La_{1-x}MnO_{3-\delta}$ phases crystallized in the rhombohedral structure showing a M–I transition, Mn-deficient phases crystallized in the orthorhombic structure and they were ferromagnetic insulators. The accommodation of excess oxygen in the so-called anion excess $LaMnO_{3+\delta}$ *via* $La_{1-x}Mn_{1-x}O_3$ was first proposed by Tofield and Scott[29] from their neutron diffraction studies. From neutron diffraction studies of $PrMnO_{3+y}$ and $NdMnO_{3+y}$, Cherepanov *et al.*[26] have shown that these oxides have A-site and Mn-site vacancies in the form of $Pr_{1-x}Mn_{1-y}O_3$ and $Nd_{1-x}Mn_{1-y}O_3$. In the present study, when a Pr to Mn ratio of 1 : 1 was taken in the preparation, compounds of the general formula $(LnA)_1Mn_{1-y}O_3$ (Ln = Pr, Nd; A = Na, K) were obtained indicating only the Mn-site vacancy. In the neutral NaCl or KCl flux method, the vacancy that could have occurred in the Pr or Nd-sites is filled by alkali ions and dissolution of excess Mn leads to the Mn-site vacancy.

The electrical and magnetic properties of Na- or K-doped $PrMnO_3$ and $NdMnO_3$ show that they are all ferromagnetic insulators. This is why mixed rare-earth manganites of the general formula $(Pr_{1-x}La_x)_{1-y}Na_yMnO_3$ were prepared to investigate the effect of structure on the electrical and magnetic properties. Clearly, the compounds crystallizing in orthorhombic structures are ferromagnetic insulators (FMI) and those crystallizing in rhombohedral structures are ferromagnetic metals (FMM).

In order to see if these Na- or K-doped oxides behave similarly to the divalent ion doped lanthanum manganites, average $\langle r_A\rangle$ values were plotted *vs.* T_c. In Fig. 7, the mean radii of the A-site, $\langle r_A\rangle$, *vs.* the ferromagnetic transition temperature, T_c, of only the stoichiometric phases from Tables 1 and 4 are plotted. Further, the data for Na and K

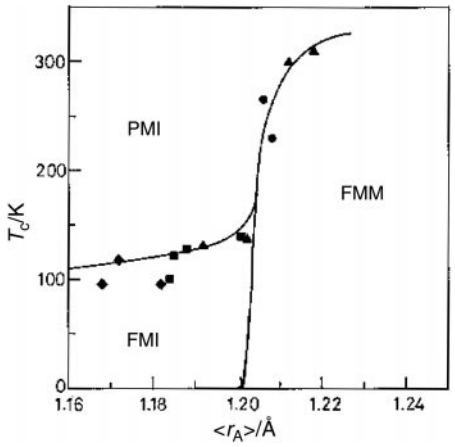

Fig. 7 Phase diagram of average radius $\langle r_A\rangle$ *vs.* ferromagnetic transition temperature, T_c, for $Pr_{1-x}A_xMnO_3$ (◆); $Nd_{1-x}A_xMnO_3$ (■); $La_{1-x}A_xMnO_3$ (●) (A = Na, K) and $(Pr_{1-x}La_x)_{1-y}Na_yMnO_3$ (▲).

doped $LaMnO_3$ from ref. 13 have been included in the plot. Average radii $\langle r_A\rangle$ values were obtained from Shannon[27] for 9-fold coordinated La^{3+}, Pr^{3+}, Nd^{3+}, Na^+ and K^+ ions. From Fig. 7, it is clear that compounds with $\langle r_A\rangle < 1.20$ Å crystallize in the orthorhombic structure and they fall in the ferromagnetic insulating region similar to the phase diagram of the divalent ion doped $La_{1-x}A_xMnO_3$ (A = Ca, Sr, Ba and Pb) system.[30] For $\langle r_A\rangle > 1.20$ Å, the compounds crystallize in the rhombohedral structure and they do show ferromagnetic metallic properties.

Conclusions

In summary, Na- or K-doped $PrMnO_3$ and $NdMnO_3$ oxides were synthesized at relatively low temperature using neutral NaCl or KCl flux. Stoichiometric Na- or K-doped oxides can be prepared when the Pr or Nd to Mn ratio is in the range of 0.8–0.9 to 1. Mn-site vacancy is indeed seen when the ratio of Pr or Nd to Mn is 1 : 1 in the preparation. These oxides crystallize in the orthorhombic structure and they are ferromagnetic insulators.

Acknowledgements

Financial support from the Department of Science and Technology, Government of India is greatly acknowledged.

References

1 G. H. Jonker and J. H. Van Santen, *Physica*, 1950, **16**, 337.
2 E. O. Wollan and W. C. Koehler, *Phys. Rev.*, 1955, **100**, 545.
3 (*a*) R. von Helmolt, J. Wecker, B. Holzapfel, L. Schultz and K. Samwer, *Phys. Rev. Lett.*, 1993, **71**, 2331; (*b*) S. Jin, T. H. Tiefel, M. McCormack, R. A. Fastnacht, R. Ramesh and H. Chen, *Science*, 1994, **64**, 413.
4 (*a*) K. Chahara, T. Ohno, M. Kasai and Y. Kozono, *Appl. Phys. Lett.*, 1993, **63**, 1990; (*b*) H. L. Ju, C. Kwon, Q. Li, R. L. Greene and T. Venkatesan, *Appl. Phys. Lett.*, 1994, **65**, 2108; (*c*) S. S. Manoharan, D. Kumar, M. S. Hegde, K. M. Sathyalakshmi, V. Prasad and S. V. Subramanyam, *J. Appl. Phys.*, 1994, **76**, 3923.
5 (*a*) R. Mahendiran, R. Mahesh, A. K. Raychaudhuri and C. N. R. Rao, *J. Phys. D*, 1995, **28**, 1743; (*b*) R. Mahendiran, R. Mahesh, A. K. Raychaudhuri and C. N. R. Rao, *Phys. Rev.*, 1996, **B53**, 12160.
6 (*a*) B. Raveau, A. Maignan and V. Caignaert, *J. Solid State Chem.*, 1995, **117**, 424; (*b*) V. Caignaert, A. Maignan and B. Raveau, *Solid State Commun.*, 1995, **95**, 357.
7 H. Kuwahara, Y. Tomioka, A. Asamitsu, Y. Moritomo and Y. Tokura, *Science*, 1995, **270**, 961.
8 (*a*) Y. Tomioka, A. Asamitsu, H. Kuwahara, Y. Moritomo and

Y. Tokura, *Phys. Rev. B*, 1996, **53**, 1689; (*b*) M. Tokunaga, N. Miura, Y. Tomioka and Y. Tokura, *Phys. Rev. B*, 1998, **57**, 5259.
9 (*a*) C. N. R. Rao, A. K. Cheetam and R. Mahesh, *Chem. Mater.*, 1996, **8**, 2421; (*b*) C. N. R. Rao, A. Arulraj, P. N. Santosh and A. K. Cheetam, *Chem. Mater.*, 1998, **10**, 2714.
10 B. Raveau, A. Maignan, C. Martin and M. Hervieu, *Chem. Mater.*, 1998, **10**, 2641.
11 (*a*) M. Itoh, T. Shimura, J. D. Yu, T. Hayashi and Y. Inaguma, *Phys. Rev. B*, 1995, **52**, 12522; (*b*) T. Shimura, T. Hayashi, Y. Inaguma and M. Itoh, *J. Solid State Chem.*, 1996, **124**, 250.
12 N. R. Washburn, A. M. Stacy and A. M. Poris, *Appl. Phys. Lett.*, 1997, **70**, 1622.
13 R. N. Singh, C. Shivakumara, N. Y. Vasanthacharya, S. Subramanian, M. S. Hegde, S. Rajagopal and A. Sequeira, *J. Solid State Chem.*, 1998, **137**, 19.
14 T. Boix, F. Sapina, Z. El-Fadli, E. Mortinez, A. Beltran, J. Veragara, R. J. Ortega and K. V. Rao, *Chem. Mater.*, 1998, **10**, 1569.
15 (*a*) Z. Jirak, J. Hejtmanek, K. Knizek and R. Sonntag, *J. Solid State Chem.*, 1997, **132**, 98; (*b*) Z. Jirak, J. Hejtmanek, E. Pollert, M. Marysko, M. Dlouha and S. Vratislav, *J. Appl. Phys.*, 1997, **81**, 5790.
16 M. Dlouha, S. Vratislav and Z. Jirak, *Physica B*, 1998, **241**, 424.
17 *Crystal growth from high temperature solutions*, eds. D. Elwell and H. J. Scheel, Academic Press, London, 1975.
18 K. Sooryanarayana, C. Shivakumara, T. N. Guru Row and M. S. Hegde, *Eur. J. Solid State Inorg. Chem.*, 1998, **35**, 273.
19 (*a*) W. H. M. Carroll, I. D. Fawcett, M. Greenblatt and K. V. Ramanujachary, *J. Solid State Chem.*, 1997, **130**, 327; (*b*) W. H. M. Carroll, I. D. Fawcett, M. Greenblatt and K. V. Ramanujachary, *J. Solid State Chem.*, 1999, **146**, 88.
20 M. Sahana, R. N. Singh, C. Shivakumara, N. Y. Vasanthacharya, M. S. Hegde, S. Subramanian, V. Prasad and S. V. Subramanyam, *Appl. Phys. Lett.*, 1997, **70**, 2909.
21 Y. Ng-Lee, F. Safina, E. Martinez-Tamayo, J. V. Folgado, R. Ibanez, D. Beltran, F. Lloret and A. Segura, *J. Mater. Chem.*, 1997, **7**, 1905.
22 (*a*) C. C. Chen and A. de Lozanne, *Appl. Phys. Lett.*, 1997, **71**, 1424; (*b*) M. Sahana, M. S. Hegde, C. Shivakumara, V. Prasad and S. V. Subramanyam, *J. Solid State Chem.*, 1999, **148**, 342.
23 C. Shivakumara, M. S. Hegde and G. N. Subbanna, *Solid State Sci.*, 2001, **3**, 43.
24 I. G. K. Andersen, E. K. Andersen, P. Norby and E. Skou, *J. Solid State Chem.*, 1994, **113**, 320.
25 A. I. Vogel, *Text book of quantitative chemical analysis*, 5th edn., Longman, England, 1989, p. 584.
26 V. A. Cherepanov, L. Y. Barkhatova, A. N. Petrov and V. I. Voronin, *J. Solid State Chem.*, 1995, **118**, 53.
27 R. D. Shannon, *Acta Crystallogr., Sect. A*, 1976, **32**, 751.
28 (*a*) J. Topfer and J. B. Goodenough, *J. Solid State Chem.*, 1997, **130**, 117; (*b*) J. Topfer and J. B. Goodenough, *Chem. Mater.*, 1997, **9**, 1467.
29 B. C. Tofield and W. C. Scott, *J. Solid State Chem.*, 1974, **10**, 183.
30 R. Mahesh, R. Mahendiran, A. K. Raychaudhuri and C. N. R. Rao, *J. Solid State Chem.*, 1995, **120**, 204.